Revisiting the protomotive vectorial motion of F_0-ATPase

Chen Bai[a,1] and Arieh Warshel[a,1,2]

[a]Department of Chemistry, University of Southern California, Los Angeles, CA 90089-1062

Contributed by Arieh Warshel, July 26, 2019 (sent for review May 30, 2019; reviewed by R. Dean Astumian and Dave Thirumalai)

The elucidation of the detailed mechanism used by F_0 to convert proton gradient to torque and rotational motion presents a major puzzle despite significant biophysical and structural progress. Although the conceptual model has advanced our understanding of the working principles of such systems, it is crucial to explore the actual mechanism using structure-based models that actually reproduce a unidirectional proton-driven rotation. Our previous work used a coarse-grained (CG) model to simulate the action of F_0. However, the simulations were based on a very tentative structural model of the interaction between subunit a and subunit c. Here, we again use a CG model but with a recent cryo-EM structure of cF_1F_0 and also explore the proton path using our water flooding and protein dipole Langevin dipole semimacroscopic formalism with its linear response approximation version (PDLD/S-LRA) approaches. The simulations are done in the combined space defined by the rotational coordinate and the proton transport coordinate. The study reproduced the effect of the protomotive force on the rotation of the F_0 while establishing the electrostatic origin of this effect. Our landscape reproduces the correct unidirectionality of the synthetic direction of the F_0 rotation and shows that it reflects the combined electrostatic coupling between the proton transport path and the c-ring conformational change. This work provides guidance for further studies in other proton-driven mechanochemical systems and should lead (when combined with studies of F_1) to a complete energy transduction picture of the F_0F_1-ATPase system.

molecular motor | ATPase | energy conversion | PTR

The generation of adenosin triphosphate (ATP) molecules by the F_0F_1-ATPase system is essential for many cellular functions (1, 2). As mentioned in ref. 3, the system includes the F_1-ATPase motor that synthesizes or hydrolyzes ATP and the membrane-bound F_0-ATPase motor that drives the mechanical rotation, utilizing the pH gradient across the membrane. The details of the conversion of energy by the F_0F_1-ATPase have long been one of the key questions in biology. Attempts to resolve this question considering the contribution of F_1-ATPase involved major progress in structural and biochemical studies as well as single-molecule spectroscopic data (4–8). Significantly, energetics of the F_1-ATPase has been analyzed by coarse-grained (CG) simulation approaches (2, 9). The studies of the action of the F_0 system will be considered below.

The general features of the F_0 system are outlined schematically in Fig. 1. As mentioned in ref. 3, it is composed of a rotor part, known as the c ring, connected to the stator subunit a and dimer subunit b (b′). The c ring is a tightly packed ring-like structure composed of several α-helical hairpins (5, 10). Most of the central part of the c ring is surrounded by the membrane, except for the loops on the stroma side and the termini on thylakoid lumen side. Each c-ring helix consists of a highly conserved Asp or Glu residue that directly bind protons or the sodium ions depending on the organism (11). Subunit a (the stator) is located adjacent to the c ring.

As mentioned in ref. 3, the structural information about F_0 includes high-resolution crystal structures of the c ring (11, 12) and a nuclear magnetic resonance solution structure (13), which only provides an hypothetical model for the c-ring–subunit a complex. All of the crystal structures of the c ring show the centrally located Asp/Glu residue in a locked conformation facing the membrane helices. New information has been provided by a recent cryogenic electron microscopy (cryo-EM) study of the cF_1F_0 structure of spinach chloroplast (14). This study yields crucial information about the position of subunit a. Several biochemical and mutational studies have highlighted the role of a highly conserved Arg residue in mediating the functional ion translocation pathways through the a–c interface. This Arg is located almost at the same level as the H^+ (Na^+) binding Asp/Glu residues in the c ring (15, 16). A schematic model of the entire F type ATP synthase (ATPase) motor is shown in Fig. 1.

Attempts to account for the action of F_0 have utilized experimental data in order to generate a workable model (5, 17–22). These studies suggested that there are different proton channels on the N (stroma) side and P (thylakoid lumen) sides of the membrane leading to release or uptake of the ion (5, 17, 20). As mentioned in ref. 3, experiments have indicated that the Arg residue blocks the uptake of ions from the low-pH reservoir (P side) after the Asp/Glu moves close to the Arg, and this forces the proton to escape to the high-pH side (N side) (16). Nevertheless, it is unclear how the pH gradient drives the rotation directionality.

Phenomenological parameters for the energy of the ionized groups were used by Oster and coworkers (21, 22). Unfortunately, the resulting models were not based on validated studies of charges in proteins. A study that considered a realistic structural model in a more explicit way (18) provided interesting insight but was based on invalidated electrostatic treatment. Furthermore, the above studies have not considered the crucial barriers for the proton transfer (PT) path and the coupling of the

Significance

The F_0F_1-adenosin triphosphate (ATP) synthase energy conversion under a proton gradient is fundamental in living cells. However, the detailed mechanism has been poorly understood due to the lack of structural information near subunit a. Here, we explored the free energy landscape of the proton transfer pathway at F_0 in the recent cryoelectron microscopy cF_1F_0 structure of spinach chloroplast ATP synthase by using our coarse-grained model. Our calculated landscape reproduced the correct unidirectionality of the rotation of F_0. It is found that the directionality is mainly due to the coupling between the change in the electrostatic energy of the c-ring conformational change and the proton transfer pathway. This work provides guidance for investigating other proton-driven mechanochemical processes.

Author contributions: C.B. and A.W. designed research, performed research, contributed new reagents/analytic tools, analyzed data, and wrote the paper.

Reviewers: R.D.A., University of Maine; and D.T., University of Texas at Austin.

Conflict of interest statement: A.W. and R.D.A. are coauthors on a 2016 review article.

[1]C.B. and A.W. contributed equally to this work.

[2]To whom correspondence may be addressed. Email: warshel@usc.edu.

First published September 11, 2019.

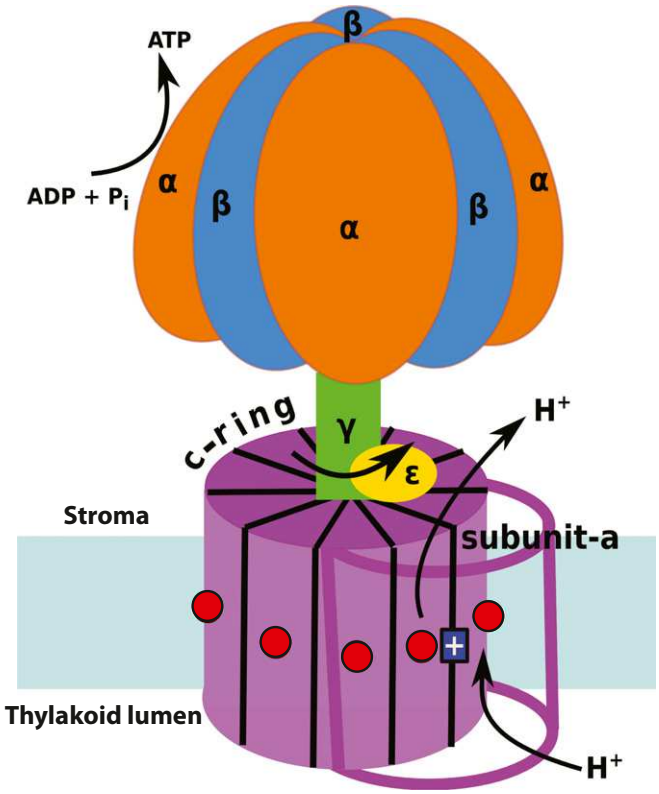

Fig. 1. A schematic diagram of the F_0F_1-ATP synthase system. The upper part consists of the α/β-catalytic subunits, and the γ stalk is the F_1-ATPase (that converts adenosine diphosphate [ADP] to ATP when the stalk rotates in the synthesis direction). The lower part is the F_0 unit, which is embedded in the membrane and includes the c-ring complexed with the stator subunit a. These units are engaged in transporting protons/cations across the membrane and in coupling this transport to the mechanical rotation of the c ring. The Glu residues, shown in red, rotate with the γ stalk, and the c ring is in the synthesis direction.

PT process with the rotary path. Moreover, the directional motion has been obtained by imposing the torque due to the ATP hydrolysis rather than modeling the torque due to the proton gradient without any phonological parameters.

Studies of the effect of the interaction between the Glu/Asp residues and the Arg should include exploration of the effect of the asymmetry on the PT path (i.e., rotation in the synthesis direction has a smaller barrier and energy than in the opposite direction). In fact, the role of such an asymmetry was thought to be the reason for the directional rotation (17). However, such studies were not based on a validated experience in modeling charges in protein interiors or on familiarity with the corresponding issue. This is exactly the issue that has been extensively studied by us (23) and exploited the electrostatic features of our CG model (24–26). At present, the CG is arguably the more reliable in assessing the negative log of the acid dissociation constant (pK_a) and electrostatic free energies in nonpolar regions of protein/membrane systems compared with the standard free energy perturbation calculations (e.g., of the type used in ref. 12) that do not involve specialized treatment of water penetration (23) or extremely long simulations.

Our previous study of the action of F_0 (3) involved converting the molecular structure of the system to a free energy map (a free energy landscape) and then, elucidating how this landscape reproduce the required vectorial process. This was done by the use of the CG model that arguably provides an optimal option for generating the needed landscape as has been successfully demonstrated for the F_1-ATPase mechanochemical coupling (9) and in the studies of other systems, including a voltage-activated proton transfer system (27).

It was found that the rotation is due to asymmetry in the energetics of the combined rotation and proton path rather than it depending only on the asymmetry of the interaction between the Asp and Arg ion pair. Our work also accounted for the free energy of the proton movement through the protein/membrane system under the effect of the pH gradient as well as the electrostatic interaction between the charges of the system along the rotational coordinate of the rotor.

However, our early work was based on very tentative structural information (13), and now, we have much more concrete structural information (14). With the structures, we can explore in greater detail the energetics of the proton transport (PTR) through the combination of both the proton transfer and the c-ring rotation.

Overall, our results reproduce the fact that the rotation of the c ring is in the synthesis direction due to the coupling of the PTR and the c-ring rotation energy landscapes.

Exploring the Proton Transport Paths

In order to explore the free energy landscape using the structural information, we utilized the recent cyro-EM structure of cF_1F_0 (14). Since our study focuses on the F_0 rotation, we trimmed the structure so that only the c ring, subunit a, and a part of subunits b and b′ were left in our model as shown in Fig. 2. The system was embedded into a 108 × 78 × 30-Å membrane, and the membrane particles were separated by 3-Å spacing. The protein dipole Langevin dipole semimacroscopic formalism with its linear response approximation version (PDLD/S-LRA) method (28) was used to calculate the PTR free energy surface. The system was modeled by several layers, where the inner layer was represented by explicit atoms and the outer layers were modeled by simplified representation. We also used our CG model (26) to perform c-ring rotation calculations. In our CG model, the main chain is in all-atom form, while the side chain is a CG particle. In all calculations, the membranes are treated by the CG model. In this method, the ionization states of the protein residues are determined by the Metropolis Monte Carlo–Proton Transfer approach (25). As in previous work, we removed part of the membrane particles near the Arg189 side chain with a cutoff with 8 Å (3). The c-ring rotation was modeled by rotating the helixes around the central axis of the ring while keeping subunits a, b, and b′ (shown in Fig. 2) fixed. From Fig. 2, Glu^- (G1) rotates in the synthesis direction (clockwise) and passes Arg^+, and G2 takes its place.

Early works (12, 18) suggested that the asymmetry of the energy profile is sufficient to account for the unidirectional rotation of c ring, and the change of polar and membrane environment plays a key role. Thus, as in the previous study, we reexamined whether the contribution from the $Glu^{(-)}$ $Arg^{(+)}$ ion pair and the membranes is sufficient to account for the unidirectional rotation of F_0. We calculated the free energy difference between the left and right c-ring rotation by using the CG method. Fig. 3 shows the rotation free energy curve for the $Glu^{(-)}$ $Arg^{(+)}$ pair when the $Glu^{(-)}$ is on either side of $Arg^{(+)}$.The calculations found that the barrier difference between the rotation to the right and the rotation to the left is relatively small (about 1.5 kcal/mol), and we cannot rule out either possibility only based on this.

Obviously, it is imperative to move from the rather simple focus on the energy of only the $Glu^{(-)}$ $Arg^{(+)}$ ion pair to a model that considers consistently the coupling of the c-ring rotation to the PTR process as well as the energetics of the PTR. To explore this issue, we used the PDLD/S-LRA approach to evaluate the energetics of a PTR between the Glu residues on the c ring and the bulk through the proton channel on either the P or N side of the c-ring–subunit a interface. However, a key element in

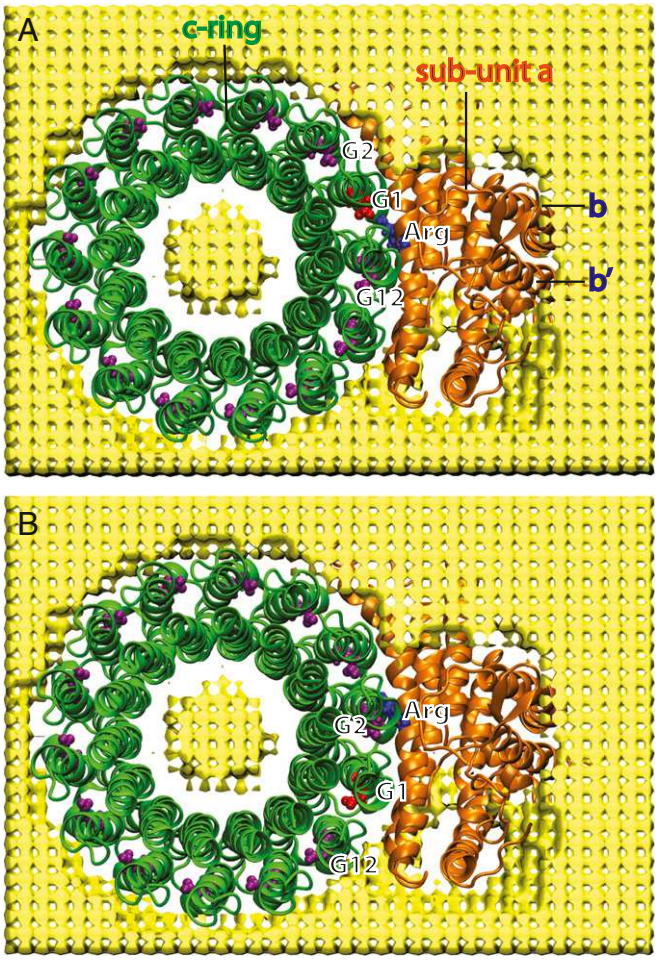

Fig. 2. Model of the F_0-ATPase. Yellow indicates the CG membrane surface. Green indicates the c ring. Orange indicates subunit a and part of subunits b and b′. Purple indicates Glu residues on c ring, and deprotonated Glu^- (G1) is in red. Blue indicates Arg189 on the c ring. The synthesis direction corresponds to clockwise rotation of the c ring. (*A*) G1 is close to Arg^+ and the PT exit channel. (*B*) The c ring is rotated in the synthesis direction, and therefore, G1 enters the membrane and is close to the PT entry channel.

this work is the implementation of our water flooding approach (29, 30) to determine the possible position of hydronium ion. This approach is particularly important in exploring the proton conductance in the membrane protein regions between the c ring and subunit a. It is also useful in exploring the conductance through the protein.

To find the proper H_3O^+ sites that define the proton channel, we first used the water flooding approach to generate the configuration of the water molecules in the gap through the possible pathways, and then, we screened all of the positions to locate the ones with relatively low energies.

Hahn et al. (14) suggested that the entry PTR go through subunit a (Fig. 4). However, our previous work has shown a PTR through the interface between subunit a and c ring is also possible as shown in Fig. 4 (3). In determining the PTR channels, we used the PDLD/S-LRA approach to calculate with the free energy change when an H_3O^+ ion is traveling along them as well as the energy-associated rotation of the c ring.

Fig. 5 depicts the free energy change through different PTR channels. Our result shows that the barrier of entry channel through subunit a is a little higher than the one through the a–c interface, but both pathways should be feasible. However, we also examined the effect of c-ring rotation on the PTR reaction. After we rotate the c ring 6° toward the synthesis direction, the energy increased by about 8 kcal/mol. This difference comes from the interaction between Arg residues on the c ring (Fig. 4) and the membrane. Fig. 6 *A*–*F* and *A*′–*F*′ clearly shows that the unidirectional rotation of F_0 is due to the free energy landscape that reflects the coupling of the PTR and the c-ring rotation. Fig. 6 *A*–*F* and *A*′–*F*′ represents the free energy change of the coupled PTR and rotation process for the synthesis direction and contrary direction, respectively. From Fig. 6*A* to Fig. 6*B*, 1 proton on G1 crossed a small barrier and is released to the N side. At this point, there are 2 Glu residues deprotonated on each side of the Arg189. Then, from Fig. 6*B* to Fig. 6*C*, the c ring rotated a little farther to right, and therefore, another Glu is able to take a proton from the P side. The transition from Fig. 6*C* to Fig. 6*D* indicates a PTR process through the entry channel, which lowers the free energy of the system by binding the proton with G12. Next, the left deprotonated G1 will pass the Arg189 with the highest barrier in this cycle. After this, the whole cycle will repeat.

However, when the c ring rotates to the left, then only 2 Glu on the c ring are protonated due to the proton binding and release mechanics as shown in Fig. 6 *A*′–*F*′. From Fig. 6*A*′ to Fig. 6*B*′, a proton is released to the N side from G1 with a small barrier. This is followed by rotation of the c ring to the left and the preparation for the next proton binding event. The rotation step from Fig. 6*B*′ to Fig. 6*C*′ has the highest barrier when G12 passes Arg189. Thus, a PTR from the P side to Glu is not very effective compared with the situation of rotation to the right as shown by Fig. 6 *C*′ and *D*′. Then, in step Fig. 6*D*′ to Fig. 6*E*′, the molecule rotates farther to the left to facilitate the next proton release to the P side, and the cycle repeats.

Fig. 6 *A*–*F* and *A*′–*F*′ shows that the barriers for the rate-determining steps for both the PTR and the rotation are smaller when the c ring rotates to the right (10.73 and 5.89 kcal/mol,

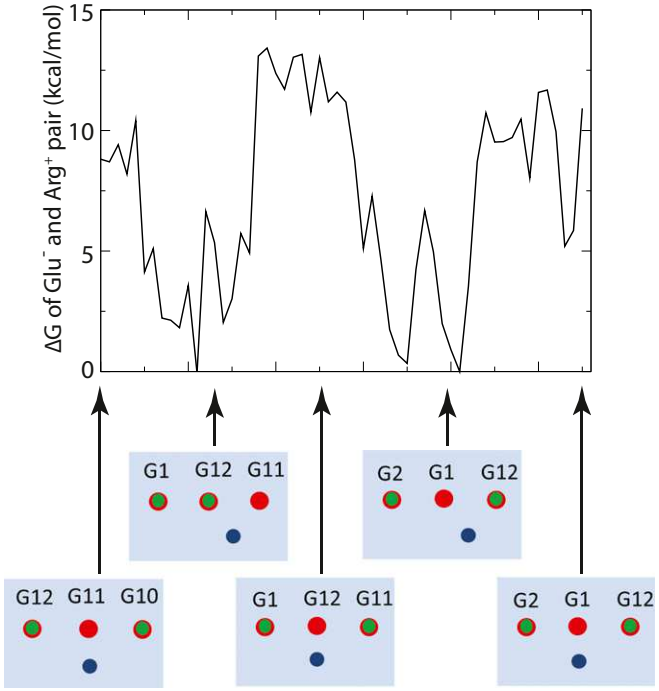

Fig. 3. The dependence of the CG free energy of the Glu^- Arg^+ ion pair on the rotation of the Glu residues of the c ring.

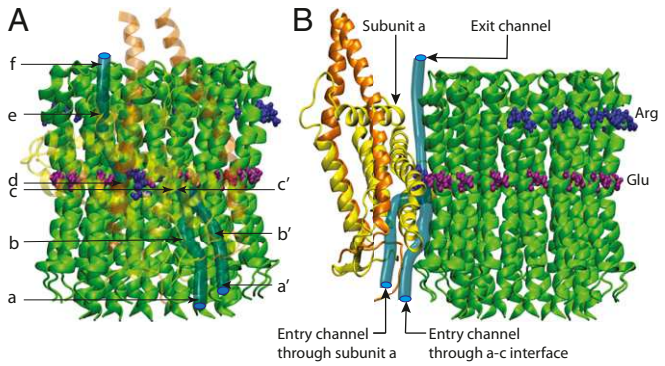

Fig. 4. Front (*A*) and side (*B*) views of the F_0-ATPase system. The cyan channels represent the PTR entry pathway through the a–c interface, through subunit a, and through the exit pathway, respectively. Subunit a is depicted in transparent yellow (for visualization convenience), while b and b′ are in transparent orange. The color codes for the other parts are the same as in Fig. 2.

respectively) compared with when it rotates to the left (13.40 and 8.17 kcal/mol, respectively). Also, the reaction energy for the cycle is more favorable for the synthesis direction (−6.29 kcal/mol) vs. the opposite direction (−2.58 kcal/mol). However, the relative positions between charged $Arg^{(+)}$ and $Glu^{(-)}$ are more electrostatically favorable (close to each other) for both the rotation and the PTR reactions when rotating to the right. These findings show that the unidirectionality of c-ring rotation is caused by the free energy landscape that is determined by the coupling of the PTR and the rotation process.

Fig. 6, *Upper* indicates that, during the conformational change of the c ring, the energy increases rapidly when a Glu residue is close to Arg189. It also shows some periodicity of the energy landscape at different rotational degrees.

Overall, the electrostatic basis of the action of F_0 can be understood intuitively by just watching the trend in the charge–charge interaction in Fig. 6. That is, in Fig. 6, we can look at the distance between the blue point representing Arg and the red points representing the ionized Glu. By doing so, we can see that more attractive interactions are going in the right direction.

Concluding Discussion

This work explores the molecular origin of the action of the F_0 proton-driven rotor. The directionality of F_0 has been tentatively ascribed to electrostatic constraints and 2 noncolinear access channels to the Arg–Glu pair (17). However, the nature of the elusive asymmetric proton channels should be based on a structural model and validated through generation of a structure-based energy landscape that considers the coupling of the PT and the F_0 c-ring rotation. This challenge has been addressed in our early work (31) that used a CG model, which was able to account for the correct direction of the vectorial process. However, our previous study was based on a very tentative structure of the a subunit. That is, the information of subunit a was lacking in the crystal structures, and a tentative structural model was generated based on an NMR solution structure, which provided a rather hypothetical model for the a–c complex.

In this work, we reexamined the action of F_0 using much more solid structural information (14) than before. Our analysis involved more careful study, which included water flooding simulations that examined in a more consistent way the energetics of the proton pathway. Two nonlinear proton entry pathways from the bulk to the c ring were found. One was through the a–c interface as indicated by our previous work (3), while another one was through subunit a as suggested by others (14). Our energy landscape calculation shows that both pathways are possible, but the one through the a–c interface has a smaller barrier.

One of the key points in our modeling approach has been the effort to generate a complete landscape that actually describes the vectorial process. This strategy that started already in our 1979 to 1981 (32, 33) works and was emphasized in several recent studies (9, 27, 34, 35) is, in our view, a crucial part in the understanding of vectorial motion.

It is useful to comment that the previous work of Walz and Caplan (19) and also, those of Oster and coworkers (21, 22) have tried to construct a phenomenological landscape. However, the relationships of these landscapes to the actual structural features are not clear. Another insightful attempt to explore the nature and the energetics of the proton path was reported by Junge and coworkers (36). This work attempted to determine the pK_a values of the groups controlling the PTR by considering current–voltage relationships and pH effects and using a minimal rotary model. The model seemed to be consistent with 2 groups of pK_a values about 6 and 10 in both sides of the membrane. However, it is very hard to obtain unique information on the PTR profile using phenomenological fitting.

When one tries to reproduce the observed directionality (i.e., the synthesis direction) by deterministic molecular models, it is not obvious that the correct direction will be reproduced. The requirement is that the calculated landscape of the combined c-ring rotation and the forward motion of the protons will have lower barriers in the synthesis direction than in the opposite direction. In such a case, the thermal Brownian motions will take the system in the correct direction. While the motion arises because of thermal noise (Brownian motion), the directionality (preference for rotating to the right rather than to the left) is due to the relative barrier heights (37). In the case of F_0, it is possible to see intuitively the origin of the unidirectionality by looking at Fig. 6 *A*–*F* and *A*′–*F*′. That is, in Fig. 6, we can look at the distance between the blue point representing Arg and the red points representing the ionized Glu. By doing so, we can see that more attractive interactions are going in the right direction. Of course, the results are given in a much more quantitative way from the energy values that connect the states in Fig. 6. The rate-determining step for rotation and PTR to the right direction (10.73 and 5.89 kcal/mol, respectively) are both lower than those to the left (13.40 and 8.17 kcal/mol, respectively). Also, the

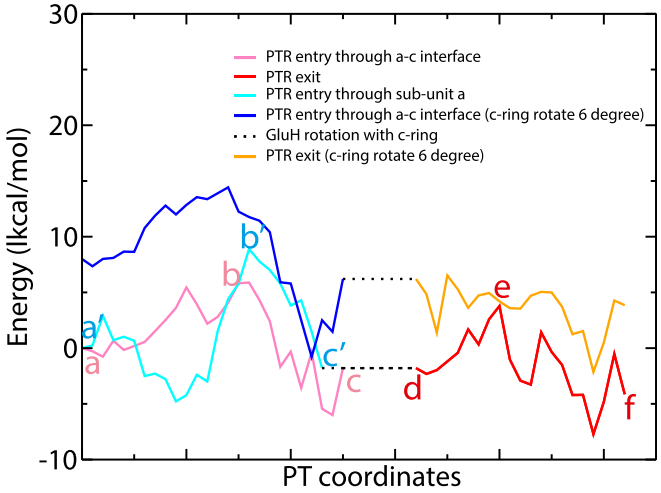

Fig. 5. The free energy change during the PTR reaction. Other than the PTR pathways shown in Fig. 4, we also examined the effect when we rotate the c ring in the synthesis direction for 6° in the first place. The energy scale includes the effect of rotating the c ring.

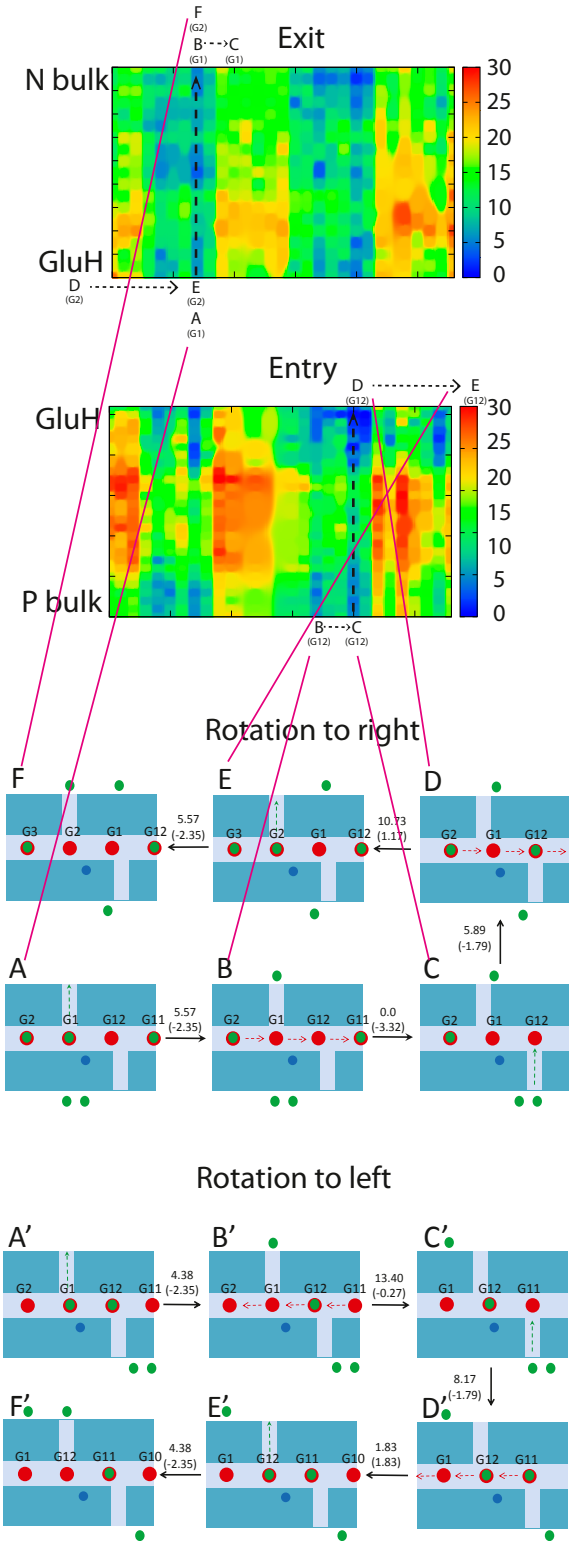

Fig. 6. The energetics of the activation of F_0. *Upper* shows the energy for the PTR/rotation in kilocalories per mole. The horizontal axis is for rotation, while the vertical axis is for a PTR from the P bulk to GluH along the entry channel through the a–c interface and from GluH to the N bulk through the exit channel as depicted in Fig. 4. The pH values for the P and N bulk regions are kept at 5 and 8, respectively. *A*–*F* and *A*′–*F*′ show schematic presentations of the PTR/rotation energetics when the c ring rotates to the synthesis direction (right) or the opposite direction, respectively. The red arrows indicate the rotation direction of the Glu residues together with c ring. The reaction free energy change of each step is next to the black arrow in parentheses together with the barrier. These states in *A*–*F* and *A*′–*F*′ are also linked to *Upper* by lines. Note that the states from *A*–*F* correspond to PTR on different Glu residues. Arg^+ is in blue, Glu^- is in red, and protons are in green.

reaction energy of the cycle for rotation to the right is lower (–6.29 kcal/mol) compared with rotation to the left (–2.58 kcal/mol). However, the relative positions between the charged Arg^+ (blue circles in Fig. 6) and Glu^- (red circles in Fig. 6) are more favorable (close to each other) for both rotation and PTR reactions when rotating to the right.

To further quantify our finding and to consider the actual kinetics that reflects the barriers and the minima, we run the kinetic program Kinetiscope (http://hinsberg.net/kinetiscope/). It was found that the population of moving to the right direction grows much faster than that to the left direction (48.5:1). It may be interesting to describe the transition state for the rate-determining step when rotating in the synthesis direction; the charge center distances between Arg^+ and H_3O^+ or between Arg^+ and the 2 closest charged Glu^- residues in the transition state for proton transfer (Fig. 6 *C* and *D*) are 22.59, 6.00, and 15.68 Å. On the contrary, the 3 distances for the transition state in the opposite rotating direction (Fig. 6 *C*′ and *D*′) are 19.89, 11.70, and 26.58 Å. The longer distance between Arg^+ and H_3O^+ and the closer distances between Arg^+ and Glu^- in synthesis direction validate that it is more electrostatically favorable.

Our conclusion that the empirical valence bond profile for PTR follows in many cases the electrostatic profile of the protonated water (23) is relevant to the $Na^{(+)}$-activated motors. That is, as mentioned in ref. 3, the profile for the $Na^{(+)}$ transfer should be similar to that of the protonated water while reflecting the difference between the energetics of the $Asp^{(-)}$ $Na^{(+)}$ and $Asp^{(-)}$ $H^{(+)}$ pairs.

One of the unique features of this strategy is the use of the water flooding approach that gives much more confidence in the position and energetics of the proton channels: in particular, in the complex regions between the subunits, the membrane, and the water surfaces.

This work and ref. 3 clarified that a proper analysis of the proton motive force that drives the rotation of F_0 rotor must include the complete landscape in both the rotation and the PTR directions. Obtaining the landscape for the F_0 rotation and combining it with our F_1-ATPase model (9) should provide a molecular model of the nature of the energy transduction in the F_0F_1-ATP synthase system.

Methods

In this work, we applied the water flooding treatment (29, 30) to reveal hydrated pathways for the PTR process. Briefly, water molecules are inserted and removed from the protein cavities following a Monte Carlo scheme until an energy minimum is reached. Subsequently, we used the PDLD/S-LRA method (28) to calculate the energy of the protons through the revealed pathways. The rotation energy of the c ring was calculated by utilizing our CG model (25, 26), which calculates the total energy of the system (see below) on the system at various constructed rotation angles. All simulations were carried out using the MOLARIS-XG package.

PDLD/S-LRA. The scaled semimacroscopic protein dipole Langevin dipole method, implemented in the MOLARIS-XG package (38, 39), computes free energies of system in bulk and in protein. This method is able to compute binding energies efficiently by constructing proper thermodynamic cycles (28). The protein dipole Langevin dipole represents water molecules as Langevin dipoles semimacroscopically. The energy is evaluated using the linear response approximation, which averages the charged and uncharged. Finally, the electrostatic energy is scaled using a dielectric constant of $\varepsilon = 4$ for the protein. For convergens, an molecular dynamics local relaxation of 0.1 ns was performed before PDLD/S-LRA calculations.

Total Energy Calculations. Our group consistently updates the CG model based on electrostatic effects in proteins and their relationship to the solvation of ionizable residues. The CG energy is defined as follows (25):

$$\Delta G^{CG}_{fold} = \Delta G^{CG}_{main} + \Delta G^{CG}_{side} + \Delta G^{CG}_{HB} = \Delta G^{CG}_{main} + \Delta G^{CG}_{elec} + \Delta G^{CG}_{hydro} + \Delta G^{CG}_{polar} + \Delta G^{CG}_{vdw} + \Delta G^{CG}_{HB}, \quad [1]$$

where the 6 energy terms represent the main-chain solvation free energy, the electrostatic free energy, the hydrophobic solvation energy, the hydrophilic (polar) solvation energy, the effective van der Waals free energy, and the effective hydrogen bond free energy, respectively. For the total energy calculation, we use the CG estimate of Eq. **1** and also apply a Monte Carlo proton transfer method (25) to evaluate the ionization state of all of the ionizable residues.

The Water Flooding Approach. Finding the correct water configuration around the binding site is very challenging, since the barriers for water penetration could be high and require very long time simulations. In the water flooding approach (29), we insert clusters of water molecules to the potential binding site; then, we optimize and evaluate the energies of the selected internal water molecules. Next, the probability of water being present at a particular position is calculated by an external Monte Carlo simulation.

ACKNOWLEDGMENTS. This work was supported by NSF Grant MCB 1707167 and NIH Grant R01-AI055926. We thank the University of Southern California High Performance Computing and Communication Center as well as the Extreme Science and Engineering Discovery Environment's Comet facility at the San Diego Supercomputing Center for computational resources.

1. P. D. Boyer, The ATP synthase–A splendid molecular machine. *Annu. Rev. Biochem.* **66**, 717–749 (1997).
2. S. Mukherjee, A. Warshel, Dissecting the role of the γ-subunit in the rotary-chemical coupling and torque generation of F1-ATPase. *Proc. Natl. Acad. Sci. U.S.A.* **112**, 2746–2751 (2015).
3. S. Mukherjee, A. Warshel, Realistic simulations of the coupling between the protomotive force and the mechanical rotation of the F0-ATPase. *Proc. Natl. Acad. Sci. U.S.A.* **109**, 14876–14881 (2012).
4. J. P. Abrahams, A. G. W. Leslie, R. Lutter, J. E. Walker, Structure at 2.8 A resolution of F1-ATPase from bovine heart mitochondria. *Nature* **370**, 621–628 (1994).
5. W. Junge, H. Sielaff, S. Engelbrecht, Torque generation and elastic power transmission in the rotary F(O)F(1)-ATPase. *Nature* **459**, 364–370 (2009).
6. J. Weber, A. E. Senior, Catalytic mechanism of F1-ATPase. *Biochim. Biophys. Acta* **1319**, 19–58 (1997).
7. H. Noji, R. Yasuda, M. Yoshida, K. Kinosita Jr, Direct observation of the rotation of F1-ATPase. *Nature* **386**, 299–302 (1997).
8. R. Shimo-Kon *et al*., Chemo-mechanical coupling in F(1)-ATPase revealed by catalytic site occupancy during catalysis. *Biophys. J.* **98**, 1227–1236 (2010).
9. S. Mukherjee, A. Warshel, Electrostatic origin of the mechanochemical rotary mechanism and the catalytic dwell of F1-ATPase. *Proc. Natl. Acad. Sci. U.S.A.* **108**, 20550–20555 (2011).
10. P. Dimroth, C. von Ballmoos, T. Meier, Catalytic and mechanical cycles in F-ATP synthases. Fourth in the cycles review series. *EMBO Rep.* **7**, 276–282 (2006).
11. T. Meier, P. Polzer, K. Diederichs, W. Welte, P. Dimroth, Structure of the rotor ring of F-Type Na+-ATPase from Ilyobacter tartaricus. *Science* **308**, 659–662 (2005).
12. D. Pogoryelov *et al*., Microscopic rotary mechanism of ion translocation in the F(o) complex of ATP synthases. *Nat. Chem. Biol.* **6**, 891–899 (2010).
13. V. K. Rastogi, M. E. Girvin, Structural changes linked to proton translocation by subunit c of the ATP synthase. *Nature* **402**, 263–268 (1999).
14. A. Hahn, J. Vonck, D. J. Mills, T. Meier, W. Kühlbrandt, Structure, mechanism, and regulation of the chloroplast ATP synthase. *Science* **360**, eaat4318 (2018).
15. R. H. Fillingame, C. M. Angevine, O. Y. Dmitriev, Coupling proton movements to c-ring rotation in F1Fo ATP synthase: Aqueous access channels and helix rotations at the a–c interface. *Biochim. Biophys. Acta* **1555**, 29–36 (2002).
16. N. Mitome *et al*., Essential arginine residue of the F(o)-a subunit in F(o)F(1)-ATP synthase has a role to prevent the proton shortcut without c-ring rotation in the F(o) proton channel. *Biochem. J.* **430**, 171–177 (2010).
17. W. Junge, H. Lill, S. Engelbrecht, ATP synthase: An electrochemical transducer with rotatory mechanics. *Trends Biochem. Sci.* **22**, 420–423 (1997).
18. A. Aksimentiev, I. A. Balabin, R. H. Fillingame, K. Schulten, Insights into the molecular mechanism of rotation in the Fo sector of ATP synthase. *Biophys. J.* **86**, 1332–1344 (2004).
19. D. Walz, S. R. Caplan, An electrostatic mechanism closely reproducing observed behavior in the bacterial flagellar motor. *Biophys. J.* **78**, 626–651 (2000).
20. S. B. Vik, B. J. Antonio, A mechanism of proton translocation by F1F0 ATP synthases suggested by double mutants of the a subunit. *J. Biol. Chem.* **269**, 30364–30369 (1994).
21. P. Dimroth, H. Wang, M. Grabe, G. Oster, Energy transduction in the sodium F-ATPase of Propionigenium modestum. *Proc. Natl. Acad. Sci. U.S.A.* **96**, 4924–4929 (1999).
22. J. Xing, H. Wang, C. von Ballmoos, P. Dimroth, G. Oster, Torque generation by the Fo motor of the sodium ATPase. *Biophys. J.* **87**, 2148–2163 (2004).
23. A. Warshel, P. K. Sharma, M. Kato, W. W. Parson, Modeling electrostatic effects in proteins. *Biochim. Biophys. Acta* **1764**, 1647–1676 (2006).
24. M. Lee, V. Kolev, A. Warshel, Validating a coarse-grained voltage activation model by comparing its performance to the results of Monte Carlo simulations. *J. Phys. Chem. B* **121**, 11284–11291 (2017).
25. I. Vorobyov, I. Kim, Z. T. Chu, A. Warshel, Refining the treatment of membrane proteins by coarse-grained models. *Proteins* **84**, 92–117 (2016).
26. S. Vicatos, A. Rychkova, S. Mukherjee, A. Warshel, An effective coarse-grained model for biological simulations: Recent refinements and validations. *Proteins* **82**, 1168–1185 (2014).
27. M. Lee, C. Bai, M. Feliks, R. Alhadeff, A. Warshel, On the control of the proton current in the voltage-gated proton channel Hv1. *Proc. Natl. Acad. Sci. U.S.A.* **115**, 10321–10326 (2018).
28. I. Muegge, H. Tao, A. Warshel, A fast estimate of electrostatic group contributions to the free energy of protein-inhibitor binding. *Protein Eng.* **10**, 1363–1372 (1997).
29. H. Yoon, V. Kolev, A. Warshel, Validating the water flooding approach by comparing it to grand canonical Monte Carlo simulations. *J. Phys. Chem. B* **121**, 9358–9365 (2017).
30. S. Chakrabarty, A. Warshel, Capturing the energetics of water insertion in biological systems: The water flooding approach. *Proteins* **81**, 93–106 (2013).
31. A. Dryga, S. Chakrabarty, S. Vicatos, A. Warshel, Realistic simulation of the activation of voltage-gated ion channels. *Proc. Natl. Acad. Sci. U.S.A.* **109**, 3335–3340 (2012).
32. A. Warshel, Conversion of light energy to electrostatic energy in the proton pump of Halobacterium halobium. *Photochem. Photobiol.* **30**, 285–290 (1979).
33. A. Warshel, Electrostatic basis of structure-function correlation in proteins. *Acc. Chem. Res.* **14**, 284–290 (1981).
34. H. Liu, Y. Shi, X. S. Chen, A. Warshel, Simulating the electrostatic guidance of the vectorial translocations in hexameric helicases and translocases. *Proc. Natl. Acad. Sci. U.S.A.* **106**, 7449–7454 (2009).
35. R. Alhadeff, A. Warshel, Reexamining the origin of the directionality of myosin V. *Proc. Natl. Acad. Sci. U.S.A.* **114**, 10426–10431 (2017).
36. B. A. Feniouk *et al*., The proton-driven rotor of ATP synthase: Ohmic conductance (10 fS), and absence of voltage gating. *Biophys. J.* **86**, 4094–4109 (2004).
37. R. D. Astumian, S. Mukherjee, A. Warshel, The physics and physical chemistry of molecular machines. *ChemPhysChem* **17**, 1719–1741 (2016).
38. S. C. L. Kamerlin, S. Vicatos, A. Dryga, A. Warshel, Coarse-grained (multiscale) simulations in studies of biophysical and chemical systems. *Annu. Rev. Phys. Chem.* **62**, 41–64 (2011).
39. F. S. Lee, Z. T. Chu, A. Warshel, Microscopic and semimicroscopic calculations of electrostatic energies in proteins by the POLARIS and ENZYMIX programs. *J. Comput. Chem.* **14**, 161–185 (1993).